

1 **Microbial Functional Gene Diversity with a Shift of Subsurface Redox Condition during *in situ***
2 **Uranium Reduction**

3
4 Yuting Liang^{1,2,3}; Joy D. Van Nostrand³; Lucie A. N'Guessan^{5,7}; Aaron D. Peacock⁴; Ye Deng³;
5 Philip E. Long⁵; C. Tom Resch⁵; Liyou Wu³; Zhili He³; Guanghe Li¹; Terry C. Hazen⁶; Derek R.
6 Lovley⁷; Jizhong Zhou^{1,3,6*}

7
8 ¹School of Environment, Tsinghua University, Beijing 100084, China

9 ²Changzhou University, Jiangsu, 213164, China

10 ³Institute for Environmental Genomics and Department of Botany and Microbiology, University of
11 Oklahoma, Norman, OK 73019

12 ⁴Center for Biomarker Analysis, University of Tennessee, Knoxville, TN 37932

13 ⁵Environmental Technology Division, Pacific Northwest National Laboratory, Richland, WA 99352

14 ⁶Earth Sciences Division, Lawrence Berkeley National Laboratory, Berkeley, CA 94720

15 ⁷Department of Microbiology, University of Massachusetts, Amherst, MA 01003

16
17 *Corresponding author: Jizhong Zhou

18 Institute for Environmental Genomics

19 University of Oklahoma

20 Norman, OK, 73019

21 Phone: (405) 325-6073

22 Fax: (405) 325-7552

23 Email: jzhou@ou.edu

24
25 Submitted to: Applied and Environmental Microbiology

26 Running title: Microbial functional diversity in U(VI) bioreduction

27 **Abstract**

28 To better understand the microbial functional diversity changes with subsurface redox conditions
29 during *in situ* uranium bioremediation, key functional genes were studied with GeoChip, a
30 comprehensive functional gene microarray, in field experiments at a uranium mill tailings remedial
31 action (UMTRA) site (Rifle, CO). The results indicated that functional microbial communities
32 altered with a shift in the dominant metabolic process as documented by hierarchical cluster and
33 ordination analyses of all detected functional genes. The abundance of *dsrAB* genes (dissimilatory
34 sulfite reductase genes) and methane generation related *mcr* genes (methyl coenzyme M reductase
35 coding genes) increased when redox conditions shifted from Fe-reducing to sulfate-reducing
36 conditions. The cytochrome genes detected were primarily from *Geobacter* sp. and decreased with
37 lower subsurface redox conditions. Statistical analysis of environmental parameters and functional
38 genes indicated that acetate, U(VI), and redox potential (E_h) were the most significant geochemical
39 variables linked to microbial functional gene structures, and changes of microbial functional
40 diversity were strongly related to the dominant terminal electron accepting process following
41 acetate addition. The study indicates that the microbial functional genes clearly reflect the *in situ*
42 redox conditions and the dominant microbial processes, which in turn influence uranium
43 bioreduction. Microbial functional genes thus could be very useful for tracking microbial
44 community structure and dynamics during bioremediation.

45 **Key words**

46 Microbial communities, GeoChip, Uranium, Sulfate-reduction, Fe-reduction, Redox condition

47

48 **Introduction**

49 Uranium contamination of groundwater, sediment and soil, initiated from uranium mining,
50 processing, storage and nuclear weapon production is a potential threat to human health and the
51 natural environment. Uranium is present in oxic to sub-oxic waters and soils primarily as soluble
52 uranyl species with high toxicity due to its bioavailability as a heavy metal and radiation source. A
53 proposed method to decrease the risk of uranium contamination is to reduce highly soluble U(VI)
54 to sparingly soluble U(IV) (17). The stimulation of microbial enzymatic reduction of U(VI) has
55 shown a substantial promise for *in situ* bioremediation of uranium contaminated groundwater,
56 where organic compounds such as acetate, ethanol or glucose were injected to the subsurface
57 environment as electron donors (1, 20, 27, 33). Multiple electron acceptors such as Mn(IV), Fe(III),
58 NO_3^- , U(VI), SO_4^{2-} in natural subsurface environments are used by microbes typically in sequence
59 of energy yield. For example, *Desulfovibrio vulgaris* showed utilization of Fe(III) first, followed by
60 U(VI) and finally sulfate in a competition experiment (6). In the field, nitrate has been shown to be
61 reduced prior to U(VI) and U(VI) reduction that often occurs simultaneously with Fe(III)
62 reduction (1, 12). However, relatively few studies have focused on functional diversity of microbial
63 communities with changes of subsurface redox conditions under *in situ* field conditions.

64 The Old Rifle site is located at a former uranium ore processing facility in Rifle, CO, where the
65 subsurface aquifer was contaminated by uranium. The site is part of the uranium mill tailings
66 remedial action (UMTRA) program of the U.S. Department of Energy. Field experiments
67 conducted at the Old Rifle site demonstrate a decrease in soluble U(VI) from groundwater upon the
68 addition of acetate to the subsurface and stimulation of endogenous microorganisms (1). Loss of
69 soluble U(VI) correlated with the stimulation of Fe-reducing conditions in the subsurface and the
70 enrichment of *Geobacter* spp., microorganisms known to reduce both Fe(III) and soluble U(VI) in
71 the subsurface (1, 10, 14, 21, 28, 30). With continuous injection of acetate, sulfate was then used by
72 microorganisms as the dominant electron acceptor. However, in some cases, an increase in U(VI)
73 concentration was observed to be associated with a shift from Fe-reducing to sulfate-reducing
74 conditions (1, 4). Thus several questions were raised regarding factors that controlled the
75 bioreduction of U(VI) and the specific microbial populations that were stimulated with shift of
76 redox conditions in the field experiments.

77 However, due to temporal and spatial changes in microbial diversity and the heterogeneity of
78 environmental conditions, characterizing the microbial communities in an accurate and
79 comprehensive way remains a challenge. The development and application of genomic tools has
80 greatly advanced characterization and profiling of the microbial communities in complex
81 environments. One such development, GeoChip 2.0 (9), is a comprehensive functional gene array.
82 The GeoChip 2.0 contains 24,243 oligonucleotide probes and covers >10,000 genes in >150
83 functional groups involved in carbon, nitrogen, phosphorus and sulfur cycling, metal reduction and
84 resistance and organic contaminant degradation, and has been demonstrated to be a robust tool for
85 investigating biogeochemical, ecological and environmental processes from different habitats (16,
86 29, 31, 36).

87 In this study, GeoChip 2.0 was used to characterize microbial communities under Fe-reducing
88 conditions and shift from Fe-reducing to sulfate-reducing conditions during *in situ* uranium
89 bioreduction. Two experimental plots were amended with acetate for stimulating microbial
90 reduction of uranium. One was maintained mainly in Fe-reducing conditions and the other
91 intentionally driven to conditions in which sulfate reduction dominated. The objectives of this study
92 were to: (i) determine the microbial functional diversity under Fe-reducing conditions and
93 transition from Fe-reducing to sulfate-reducing conditions and (ii) link geochemical changes to
94 microbial functional diversity. Our results demonstrate a shift in the functional structure of
95 microbial communities from Fe-reducing to sulfate-reducing conditions. The microbial community
96 structure and functional dynamics changed in a manner consistent with geochemical differences
97 associated with different redox conditions.

98 **Materials and Methods**

99 *Site description and plot design*

100 The Old Rifle UMTRA site is a flood plain of the Colorado River consisting of recent alluvium
101 overlying the Eocene Wasatch Formation. The flood plain is approximately 2 km long, and
102 virtually the entire site was contaminated as a result of a long-term vanadium and uranium milling
103 operation. The groundwater flows at 0.46 to >0.61 m/day in a direction that normally parallels the
104 Colorado River. The geology and hydrogeology of the site were described previously (1, 3, 4, 20,
105 28). In this experiment, two adjacent experimental plots of background, injection and

106 down-gradient wells, one installed in 2004 and the other in 2005, were run simultaneously. The
107 experimental plots had similar layouts with the 2005 experimental plot, 3.8 m to the southeast.
108 Each experimental plot had five injection wells perpendicular to groundwater flow, four monitoring
109 wells down-gradient of acetate injection, and one monitoring well positioned up-gradient of the
110 injection wells (4) (Figure 1). The 2004 experimental plot was amended with acetate for about
111 three-weeks to introduce Fe-reducing conditions. Amendment to the 2005 experimental plot was
112 started earlier and the subsurface was driven to sulfate-reducing conditions. Injections to both
113 experimental plots were stopped simultaneously on September 19, 2006.

114 *Sampling*

115 Groundwater were sampled and analyzed from July 17 to October 31 in the two experimental plots
116 (4). Groundwater (2 liters) was collected in sterile glass bottles using a peristaltic pump and kept on
117 ice until it was delivered to the laboratory and then filtered (0.2 μm) to collect biomass. Filters were
118 stored at -80 °C until DNA extraction. To better understand the microbial functional structure with
119 subsurface redox changes, 8 groundwater samples, B05 (7/27, 9/16), M16 (9/5, 9/19) M21 (7/27,
120 8/10) and M24 (7/27, 8/10) were selected for microbial functional structure analysis with GeoChip.
121 The 9/5 sample and 9/19 sample (M16) corresponded to the early days and the end of acetate
122 injection in the 2004 experimental plot, where there was a continuous decrease of redox potential
123 (E_h) under Fe-reducing condition. The 7/27 and 8/10 sample set (M21, and M24) corresponded to
124 the shift from iron-reducing to sulfate-reducing conditions in the 2005 experimental plot. The
125 samples of B05 were used as background control. Groundwater was pumped from the designated
126 depth(s) in the monitoring wells using a portable peristaltic pump (ColePalmer Instrument Co.).
127 The geochemical analysis of U(VI), Fe(II), bromide (potassium bromide as tracer), acetate, sulfate
128 and molecular analysis was described previously (4). The pH, dissolved oxygen (DO), sulfide,
129 conductivity and the redox potential of groundwater were determined in the field (4). Since only
130 trace level of nitrate was detected previously (1, 3), it was not considered in this experiment.

131 *DNA isolation and purification*

132 Community DNA was extracted from groundwater filters by combining grinding and SDS for cell
133 lysis and purified as detailed in Zhou *et al* (35). Purification was modified by elution of DNA from

134 the resin column two times with 30 μ l of hot water (80 $^{\circ}$ C). The purified DNA was quantified with
135 an ND-1000 spectrophotometer (Nanodrop Inc.) and Quant-ItTM PicoGreen[®] (Invitrogen, Carlsbad,
136 CA).

137 *Sample amplification, labeling, microarray hybridization and data processing*

138 An aliquot of DNA (25 ng) of each sample was amplified in triplicate using the TempliPhi kit
139 (Amersham Biosciences, Piscataway, NJ) and labeled as described previously (31, 32).
140 Hybridizations were performed with GeoChip 2.0 (9) on an HS4800 Pro Hybridization Station
141 (TECAN US, Durham, NC, USA) in triplicate at 45 $^{\circ}$ C for 10 hrs. Microarrays were scanned on a
142 ScanArray5000[®] Microarray Analysis System (PerkinElmer, Wellesley, MA) at 95% laser power
143 and 68% PMT (photomultiplier tube gain). Signal intensities were measured with ImaGene 6.0
144 (Biodiscovery Inc., El Segundo, CA, USA). Background was subtracted from all intensity data used
145 for further analysis. Intensities of three replicates for each set of experiments were normalized with
146 total intensities of all spots with signal-to-noise ratio (SNR; SNR = (signal intensity - background
147 intensity)/background standard deviation) greater than 1.0. Spots with SNR <2.0 and outliers of
148 replicates (>2 standard deviation) were removed. A gene was included in the analysis when a
149 positive hybridization signal was obtained from >34% of the spots (generally, 9 spots for each gene)
150 on the arrays in triplicate hybridizations. The microarray data presented are available at
151 <http://ieg.ou.edu/4download/>.

152 *Statistical analysis*

153 Cluster analysis was performed using the pairwise average-linkage hierarchical clustering
154 algorithm (5) in CLUSTER (<http://rana.stanford.edu>), and the results of hierarchical clustering were
155 visualized using TREEVIEW (<http://rana.stanford.edu/>). Bio-Env procedure was used to select
156 environmental variables to find the best subset of environmental variables with maximum (rank)
157 correlation with community dissimilarities (15) in R version 2.11.1 with vegan package. Canonical
158 correspondence analysis (CCA) was performed to identify the relationship between geochemical
159 parameters and microbial functional genes using CANOCO for Windows Version 4.5 (25). Monte
160 Carlo tests were used to assess the significance of the environmental variables with 999
161 permutations. Mantel test was performed to infer the correlation between geochemistry and

162 functional genes based on Euclidean distance measurement with PC-ORD (MjM Software,
163 Glenden Beach, Oregon, USA). The *P*-value of the standardized Mantel statistic (*r*) was calculated
164 from 999 Monte Carlo randomizations. All analyses of variances (13) were performed with SPSS
165 13.0 (SPSS Inc. Chicago, IL) with Kruskal-Wallis test and variance homogeneity by Levene's test
166 first.

167 **Results and Discussion**

168 *Field geochemical changes*

169 Geochemical analysis of the eight samples from four wells with different time points were selected
170 for this study (acetate, U(VI), sulfate, sulfide, Fe(II), DO, pH, conductivity and redox potential)
171 (Table 1). U(VI) concentrations in the background well and the two experimental plots were as
172 high as 1.0 ~ 1.5 μM . There was a continuing decrease of U(VI) with acetate injection in the 2004
173 experimental plot, and the concentration was lowered to 0.19 μM on September 19. In the 2005
174 experimental plot (M21 and M24), the U(VI) concentration decreased firstly, while there was a
175 rebound of U(VI) with a shift of subsurface redox condition from Fe-reducing to sulfate-reducing
176 conditions (4). In the same wells, there was a loss of sulfate and an accumulation of sulfide when
177 they were dominated by sulfate-reducing conditions.

178 Acetate additions were used to stimulate U(VI) reduction at the Rifle site, CO (1, 4, 28, 34).
179 At that site, continuous U(VI) reduction was observed until dominant microbial communities
180 shifted from Fe-reducing bacteria to sulfate-reducing bacteria, at which point U(VI) reduction
181 slowed, ceased or rebound (1, 4). Furthermore, the greatest rate of reduction of uranium was
182 observed under Fe-reducing conditions, consistent with previous work showing that Fe-reducing
183 conditions were more favorable for uranium reduction in a laboratory bioreduction experiment (2).

184 *Overall functional gene diversity pattern*

185 To track the microbial community dynamics during biostimulation, functional genes from selected
186 samples in the unstimulated background (B05), Fe-reducing dominance (M16) and a transition
187 from Fe-reducing to sulfate-reducing condition (M21 and M24) wells were analyzed with GeoChip
188 2.0. More than 1300 genes showed positive hybridization signals. Hierarchical cluster analysis of
189 all detected functional genes was performed (Figure 2). The cluster analysis indicated that samples

190 in treatment wells (M16, M21, M24) and background well (B05) grouped separately, except the
191 sample in the early days of acetate injection in well M21 (Figure 2(a)). Samples in treatment wells
192 grouped together mainly by Fe- or sulfate-reducing conditions, consistent with the expected
193 correlation of the dominant terminal electron accepting process with microbial functional structure
194 (Figure 2(a)).

195 From the functional gene cluster results, a total of six major groups were observed (Figure
196 2(b)). Groups 1 and 5 represented genes in high abundance under the beginning and the end of
197 Fe-reducing conditions, respectively. These groups mainly contained metal resistance and reduction
198 genes such as chromium-, arsenic-, and tellurium- related genes as well as cytochrome genes.
199 Groups 2 and 3 represented genes in high abundance in M21 7/27, which was closer to the injection
200 well and referred to the transition from Fe-reducing to sulfate-reducing conditions, of which many
201 sulfate-reducing genes (*dsrA* and *dsrB*) were observed. Group 3, 4, and 6 represented genes in high
202 abundance in the background wells. These groups of genes were mainly involved in carbon
203 degradation, nitrogen cycling and metal resistance. These results suggest that the overall functional
204 structure of microbial communities is different with subsurface redox changes, and that they were
205 also different from those in the background well.

206 The composition of microbial communities was further analyzed in nine functional categories:
207 carbon degradation, carbon fixation, sulfate reduction, metal reduction and resistance, nitrogen
208 fixation, nitrification, nitrogen reduction, organic contaminant remediation, and methane generation
209 (Figure 3). Microbial functional gene patterns at the beginning and at the end of the study period in
210 the background well were quite similar (B05 7/27, B05 9/19). Metal reduction genes increased
211 under Fe-reducing conditions (M16) over time. A previous study also showed that metal-reducing
212 δ -Proteobacteria increased from 5% to nearly 40% by analyzing 16S rRNA gene clone libraries in
213 contaminated subsurface sediments (22). The stimulation of both Fe-reducing bacteria and their
214 metal reducing related genes plays an important role in enzymatic uranium reduction.

215 When redox condition shifted from Fe- to sulfate-reducing conditions, an increase in the
216 abundance of sulfate reduction genes (*dsrA* and *dsrB*) was observed in M21 and M24, respectively
217 (Figure 3). Simultaneously, methane generation genes increased during redox transition period in
218 both M21 and M24 (Figure 3). This transition was also observed that microbial communities
219 shifted from predominance by metal-reducing *Geobacteraceae* populations to sulfate-reducing

220 *Desulfovibrionaceae* (11). It was hypothesized that the decrease in U(VI) removal efficiency was
221 due to a loss in the metal-reducing population (i.e., *Geobacter*) with a depletion of the bioavailable
222 Fe(III) concentration, suggesting that redox conditions should be optimized for continued growth
223 and survival of *Geobacter* species for long-term *in situ* uranium reduction (1).

224 ***Representatives of functional genes detected under Fe- and sulfate-reducing conditions***

225 *(i) Cytochrome genes for metal reduction*

226 Biogeochemical and genetic studies both indicate that c-type cytochromes are required for U(VI)
227 reduction by a range of microorganisms including *Desulfovibrio* sp. (18), *Geobacter* sp. (23), and
228 *Shewanella oneidensis* MR-1 (19). Here, we examine the cytochrome genes detected during
229 uranium reduction under Fe-reducing conditions and transition from Fe-reducing to
230 sulfate-reducing conditions, as visualized by clustering analysis (Figure 4). The cytochrome genes
231 showed significant correlations ($r = 0.71$, $P = 0.016$) with uranium concentrations based on the
232 Mantel test. And cytochrome genes decreased during subsurface redox conditions shifted from
233 Fe-reducing to sulfate-reducing conditions, consistent with the hypotheses that c-type cytochromes
234 are directly involved in U(VI) reduction and that a decrease of U(VI) in groundwater is greatest
235 under Fe-reducing conditions. The c-type cytochrome genes appear to be derived mainly from
236 *Geobacter* sp. and *Desulfovibrio* sp., and major groups of cytochrome genes across all samples
237 were from *Geobacter sulfurreducens* (Figure 4), whose c-type cytochromes have been shown to be
238 involved in extracellular uranium reduction (23).

239 *(ii) dsrA/B for sulfate reduction*

240 To examine the shift of a microbial community composition dominated by sulfate reducers in more
241 detail, total *dsr* genes were analyzed. In well M16, the number of *dsr* genes decreased when it was
242 driven to Fe-reducing conditions, while in wells M21 and M24, it increased with shift to
243 sulfate-reducing conditions (Table S1). The diversity increased in well M21 during sulfate
244 reduction, most of the genes (95%) could be found in samples collected before and after acetate
245 injection (Table S2). Also, *dsr* genes in M21 showed a high similarity with those in the background
246 well (92%-97%). Hierarchical clustering was performed to assess the *dsr* gene patterns (Figure S1).
247 Compared to the Fe-reducing conditions, an obvious increase of *dsr* genes was detected when the

248 subsurface was dominated by sulfate reduction. The *dsr* genes came from both cultured bacteria
249 (e.g., *Desulfomonile* sp., *Desulfosporosinus* sp., *Desulfotomaculum* sp., *Desulfovibrio* sp.,
250 *Desulfovirga* sp. and *Chlorobium* sp.) and uncultured sulfate-reducing bacteria in well M21 at the
251 late sampling date (8/10/06), when the sulfide concentration was highest. Several *dsr* genes from
252 uncultured sulfate-reducing bacteria similar to *Desulfosporosinus* sp. and *Pelotomaculum* sp. were
253 abundant in all samples.

254 (iii) *mcr* for methane generation

255 In the background well, *mcr* genes were mainly derived from uncultured archaeon and
256 *Methanothermobacter* sp. (Figure S2). An increase of total signal intensity of methane generation
257 genes (*mcrA*, *mcrG*, *mcrC*, *mcrD*) were observed in the well M21 7/27 in comparison to the
258 background well (B05). Methane concentrations would need to be measured during biostimulation
259 to confirm this. The increasing *mcr*-containing populations detected included primarily
260 *Methanoculleus* sp., *Methanocorpusculum* sp., *Methanocaldococcus* sp., *Methanothermobacter* sp.,
261 *Methanopyrus* sp., and uncultured archaea.

262 (iv) *nirS/K*, and *nifH* for nitrogen cycling

263 Functional genes *nirS*, *nirK* and *nifH* coding key enzymes involved in denitrification and nitrogen
264 fixation, respectively were examined. The nitrogen reducing genes, *nirS* and *nirK* genes, were
265 present under both redox conditions as well as in the background well (Figure S3). It has been
266 recognized that nitrogen reducing bacteria are essential for the removal of nitrate to create the
267 low-redox conditions favorable for U(VI) reduction (26, 7). Since only trace level of nitrate was
268 detected in the Old Rifle site (1, 3), no clear relationship between nitrogen reducing genes and the
269 redox conditions was observed in this study. These genes were likely derived from populations of
270 *Pseudomonas* sp., *Sinorhizobium* sp., *Nitrosomonas* sp., *Ochrobactrum* sp., and *Paracoccus* sp., yet
271 the majority of the nitrogen cycling genes was from uncultured bacteria. Similarly, most of the *nifH*
272 genes observed were from uncultured bacteria (Figure S4).

273 (v) Carbon degradation related genes

274 A variety of carbon degradation genes were detected in the samples (Figure S5). The functional
275 genes for cellulase from *Leuconostoc* sp., chitinase from *Salinivibrio* sp., *Burkholderia* sp., and

276 laccase from *Trametes* sp., were detected across all samples. Additionally, genes for cellulase from
277 *Clostridium* sp. and *Gluconacetobacter* sp., chitinase from *Serratia* sp., *Xanthomonas* sp., and
278 *Burkholderia* sp., and polygalacturonase gene (*pgl*) from *Penicillium* sp., were highly abundant in
279 the background well. In the Fe-reducing well, genes for cellulase from *Neurospora* sp.,
280 *Reticulitermes* sp., *Clostridium* sp., *Xanthomonas* sp., and *Fusarium* sp., chitinase from *Aeromonas*
281 sp., laccase from *Trametes* sp., *Basidiomycete* sp., and *pgl* from *Xanthomonas* sp., were also highly
282 abundant. In the sulfate-reducing well, the cellulase genes from *Clostridium* sp., *Fusarium* sp.,
283 *Halobacterium* sp., and *Gluconacetobacter* sp., chitinase genes from *Serratia* sp., *Xanthomonas* sp.,
284 and *Microbulbifer* sp., mannanase gene from *Cellvibrio* sp., and *pgl* from *Xanthomonas* sp., were in
285 a high abundance. Several different species of *Clostridium* have been shown to reduce U(VI) to
286 U(IV) to various degrees (2, 24) and the hypothesis was proposed that U(VI) reduction occurred
287 through hydrogenases and other enzymes (8). However, hydrogenase genes derived from
288 *Clostridium* sp. were not contained on the GeoChip and further work is required to confirm the
289 mechanism of bioreduction of U(VI) by *Clostridium* sp. Detrital organic matter that is locally
290 abundant at the Rifle site is probably the principal source of carbon compounds sustaining this part
291 of the microbial community.

292 ***Linking geochemistry and microbial community structure***

293 The responses of the microbial community to subsurface redox conditions can be very different
294 based on the local environmental conditions and the biostimulation operations (i.e., exogenous
295 substrate injection) (26). Bio-Env procedure was used to find the best subset of environmental
296 variables with maximum (rank) correlation with community dissimilarities and the result indicated
297 that acetate, U(VI) and E_h had the highest correlation coefficient ($r = 0.579$). Canonical
298 correspondence analysis (CCA) was performed to discern possible linkages between geochemical
299 parameters and microbial community functional structure (Figure 5). Only geochemical parameters
300 that were significant were included in the CCA biplot (acetate, U(VI), sulfate, sulfide, Fe(II), E_h),
301 based on a forward selection procedure and variance inflation factors with 999 Monte Carlo
302 permutations. For all functional genes, 37.1% of the total variance could be explained by the first
303 two constrained axes with the first axis explaining 19.5%. The specified model was significant
304 (first axis, $P = 0.019$; all axes, $P = 0.040$). The CCA results reflected the microbial functional

305 distributions along the environmental variables such as U(VI), acetate, E_h , sulfate, sulfide and Fe(II)
306 (Figure 5). B05 samples distributed in the area with highest U(VI). In the Fe-reducing well (M16),
307 the change of microbial structure was correlated with E_h . With continuous decrease of E_h and
308 accumulation of sulfide, a clear shift of microbial structure was observed with transition from
309 Fe-reducing to sulfate-reducing conditions (wells M21 and M24, from 7/27 to 8/10). The results
310 here indicated that changes of microbial functional diversity were strongly related to the dominant
311 terminal electron accepting process following acetate addition.

312 In summary, this study characterized the functional structure and dynamics of microbial
313 communities under Fe-reducing and sulfate-reducing conditions during *in situ* U(VI) bioreduction.
314 Analysis of key functional genes indicated a shift of functional potential of microbial communities
315 in response to the transition from Fe-reduction to sulfate reduction as the dominant terminal
316 electron accepting process. As a result, an increase of *dsr* and *mcr* genes was detected when the
317 subsurface was dominated by sulfate-reducing conditions. Also, the c-type cytochrome genes
318 detected were primarily from *Geobacter* sp. and *Desulfovibrio* sp. and decreased during subsurface
319 redox conditions shifted from Fe-reducing to sulfate-reducing conditions. Overall, microbial
320 functional structure is sensitive to changes in subsurface redox conditions, indicating that tracking
321 microbial functional genes could be very useful for tracking microbial community structure and
322 dynamics during bioremediation.

323 **Acknowledgements**

324 This research was supported by the Office of Science, Office of Biological and Environmental
325 Research, of the U. S. Department of Energy under Contract No. DE-AC02-05CH11231 as part of
326 ENIGMA, the Oklahoma Center for the Advancement of Science and Technology under Oklahoma
327 Applied Research Support Program, State Key Joint Laboratory of Environment Simulation and
328 Pollution Control (Grant 11Z03ESPCT) at Tsinghua University, National Natural Scientific
329 Foundation of China (No. 40730738, No. 41101233) and Natural Scientific Foundation of Jiangsu
330 province (No. BK2011233). The field experiment and biogeochemical sample analyses were

331 supported by the U. S. Department of Energy under the Environmental Remediation Sciences
332 Program.

333 References

- 334 1. **Anderson, R., H. Vrionis, I. Ortiz-Bernad, C. Resch, P. Long, R. Dayvault, K. Karp, S.**
335 **Marutzky, D. Metzler, A. Peacock, D. White, M. Lowe, and D. Lovley.** 2003.
336 Stimulating the *in situ* activity of *Geobacter* species to remove uranium from the
337 groundwater of a uranium-contaminated aquifer. *Appl Environ Microb* **69**:5884-5891.
- 338 2. **Boonchayaanant, B., D. Nayak, D. Xin, and C. Criddle.** 2009. Uranium reduction and
339 resistance to reoxidation under iron-reducing and sulfate-reducing conditions. *Water Res*
340 **43**:4652-4664.
- 341 3. **Chang, Y., P. Long, R. Geyer, A. Peacock, C. Resch, K. Sublette, S. Pfiffner, A.**
342 **Smithgall, R. Anderson, H. Vrionis, J. Stephen, R. Dayvault, I. Ortiz-Bernad, D.**
343 **Lovley, and D. White.** 2005. Microbial incorporation of C-13-labeled acetate at the field
344 scale: Detection of microbes responsible for reduction of U(VI). *Environ Sci Technol*
345 **39**:9039-9048.
- 346 4. **Druhan, J., M. Conrad, K. Williams, A. N'Guessan, P. Long, and S. Hubbard.** 2008.
347 Sulfur isotopes as indicators of amended bacterial sulfate reduction processes influencing
348 field scale uranium bioremediation. *Environ Sci Technol* **42**:7842-7849.
- 349 5. **Eisen, M., P. Spellman, P. Brown, and D. Botstein.** 1998. Cluster analysis and display of
350 genome-wide expression patterns. *Proc Natl Acad Sci USA* **95**:14863-14868.
- 351 6. **Elias, D., J. Sufita, M. McNerney, and L. Krumholz.** 2004. Periplasmic cytochrome c(3)
352 of *Desulfovibrio vulgaris* is directly involved in H₂-mediated metal but not sulfate
353 reduction. *Appl Environ Microb* **70**:413-420.
- 354 7. **Finneran, K. T., M. Housewright, and D. R. Lovley.** 2002. Multiple influences of nitrate
355 on uranium solubility during bioremediation of uranium-contaminated subsurface sediments.
356 *Environ Microbiol* **4**:510-516.
- 357 8. **Gao, W., and A. Francis.** 2008. Reduction of uranium(VI) to uranium(IV) by *Clostridia*.
358 *Appl Environ Microb* **74**:4580-4584.
- 359 9. **He, Z., T. Gentry, C. Schadt, L. Wu, J. Liebich, S. Chong, Z. Huang, W. Wu, B. Gu, P.**
360 **Jardine, C. Criddle, and J. Zhou.** 2007. GeoChip: a comprehensive microarray for
361 investigating biogeochemical, ecological and environmental processes. *ISME J* **1**:67-77.
- 362 10. **Holmes, D., R. O'Neil, H. Vrionis, L. N'Guessan, I. Ortiz-Bernad, M. Larrahondo, L.**
363 **Adams, J. Ward, J. Nicoll, K. Nevin, M. Chavan, J. Johnson, P. Long, and D. Lovley.**
364 2007. Subsurface clade of Geobacteraceae that predominates in a diversity of
365 Fe(III)-reducing subsurface environments. *ISME J* **1**:663-677.
- 366 11. **Hwang, C., W. Wu, T. Gentry, J. Carley, G. Corbin, S. Carroll, D. Watson, P. Jardine,**
367 **J. Zhou, C. Criddle, and M. Fields.** 2009. Bacterial community succession during *in situ*
368 uranium bioremediation: spatial similarities along controlled flow paths. *ISME J* **3**:47-64.
- 369 12. **Istok, J., J. Senko, L. Krumholz, D. Watson, M. Bogle, A. Peacock, Y. Chang, and D.**
370 **White.** 2004. *In situ* bioreduction of technetium and uranium in a nitrate-contaminated
371 aquifer. *Environ Sci Technol* **38**:468-475.

- 372 13. **Ivanova, I., J. Stephen, Y. Chang, J. Brüggemann, P. Long, J. McKinley, G.**
373 **Kowalchuk, D. White, and S. Macnaughton.** 2000. A survey of 16S rRNA and amoA
374 genes related to autotrophic ammonia-oxidizing bacteria of the beta-subdivision of the class
375 proteobacteria in contaminated groundwater. *Can J Microbiol* **46**:1012-1020.
- 376 14. **Komlos, J., H. S. Moon, and P. R. Jaffe.** 2008. Effect of sulfate on the simultaneous
377 bioreduction of iron and uranium. *J Environ Qual* **37**:2058-2062.
- 378 15. **K. R. Clarke, M. Ainsworth.** 1993. A method of linking multivariate community structure
379 to environmental variables. *Mar Ecol Prog Ser* **92**: 205-219.
- 380 16. **Liang, Y., D. V. J. Nostrand, Y. Deng, Z. He, L. Wu, X. Zhang, G. Li, and J. Zhou.**
381 2011. Functional gene diversity of soil microbial communities from five oil-contaminated
382 fields in China. *ISME J* **5**:403-413.
- 383 17. **Lovley, D., E. Phillips, Y. Gorby, and E. Landa.** 1991. Microbial reduction of uranium.
384 *Nature* **350**:413-416.
- 385 18. **Lovley, D., P. Widman, J. Woodward, and E. Phillips.** 1993. Reduction of uranium by
386 cytochrome-c(3) of *Desulfovibrio vulgaris*. *Appl Environ Microb* **59**:3572-3576.
- 387 19. **Marshall, M., A. Beliaev, A. Dohnalkova, D. Kennedy, L. Shi, Z. Wang, M. Boyanov, B.**
388 **Lai, K. Kemner, J. McLean, S. Reed, D. Culley, V. Bailey, C. Simonson, D. Saffarini,**
389 **M. Romine, J. Zachara, and J. Fredrickson.** 2006. c-Type cytochrome-dependent
390 formation of U(IV) nanoparticles by *Shewanella oneidensis*. *Plos Biol* **4**:1324-1333.
- 391 20. **N'Guessan, A., H. Vrionis, C. Resch, P. Long, and D. Lovley.** 2008. Sustained removal
392 of uranium from contaminated groundwater following stimulation of dissimilatory metal
393 reduction. *Environ Sci Technol* **42**:2999-3004.
- 394 21. **N'Guessan, A. L., H. Elifantz, K. P. Nevin, P. J. Mouser, B. Methe, T. LWoodard, K.**
395 **Manley, K. H. Williams, M. J. Wilkins, J. T. Larsen, P. E. Long, and D. R. Lovley.**
396 2010. Molecular analysis of phosphate limitation in *Geobacteraceae* during the
397 bioremediation of a uranium-contaminated aquifer. *ISME J* **4**:253-266.
- 398 22. **North, N., S. Dollhopf, L. Petrie, J. Istok, D. Balkwill, and J. Kostka.** 2004. Change in
399 bacterial community structure during *in situ* Biostimulation of subsurface sediment
400 cocontaminated with uranium and nitrate. *Appl Environ Microb* **70**:4911-4920.
- 401 23. **Shelobolina, E., M. Coppi, A. Korenevsky, L. DiDonato, S. Sullivan, H. Konishi, H. Xu,**
402 **C. Leang, J. Butler, B. Kim, and D. Lovley.** 2007. Importance of c-type cytochromes for
403 U(VI) reduction by *Geobacter sulfurreducens*. *BMC Microbiol* **7**:16.
- 404 24. **Tebo, B., and A. Obratzsova.** 1998. Sulfate-reducing bacterium grows with Cr(VI), U(VI),
405 Mn(IV), and Fe(III) as electron acceptors. *FEMS Microbiol Lett* **162**:193-198.
- 406 25. **ter Braak, C. J. F., Smilauer, P.** 1998. CANOCO reference manual and user's guide to
407 CANOCO for windows: software for canonical community ordination, Version 4ed.
408 Microcomputer Power, New York.
- 409 26. **Van Nostrand, J. D., L. Wu, W. M. Wu, Z. Huang, T. Gentry, Y. Deng, J. Carley, Z.**
410 **He, B. Gu, J. Luo, C. Criddle, D. Watson, P. Jardine, T. L. Marsh, J. M. Tiedje, T.**
411 **Hazen, and J. Zhou.** 2011. Dynamics of microbial community composition and function
412 during *in situ* bioremediation of a uranium-contaminated aquifer. *Appl Environ Microb*
413 **77**:3860-3869.
- 414 27. **Van Nostrand, J. D., W. M. Wu, L. Y. Wu, Y. Deng, J. Carley, S. Carroll, Z. L. He, B.**
415 **H. Gu, J. Luo, C. S. Criddle, D. B. Watson, P. M. Jardine, T. L. Marsh, J. M. Tiedje, T.**
416 **C. Hazen, and J. Z. Zhou.** 2009. GeoChip-based analysis of functional microbial

- 417 communities during the reoxidation of a bioreduced uranium-contaminated aquifer. *Environ*
 418 *Microbiol* **11**:2611-2626.
- 419 28. **Vrionis, H., R. Anderson, I. Ortiz-Bernad, K. O'Neill, C. Resch, A. Peacock, R.**
 420 **Dayvault, D. White, P. Long, and D. Lovley.** 2005. Microbiological and geochemical
 421 heterogeneity in an in situ uranium bioremediation field site. *Appl Environ Microb*
 422 **71**:6308-6318.
- 423 29. **Wang, F., H. Zhou, J. Meng, X. Peng, L. Jiang, P. Sun, C. Zhang, J. Van Nostrand, Y.**
 424 **Deng, Z. He, L. Wu, J. Zhou, and X. Xiao.** 2009. GeoChip-based analysis of metabolic
 425 diversity of microbial communities at the Juan de Fuca Ridge hydrothermal vent. *Proc Natl*
 426 *Acad Sci USA* **106**:4840-4845.
- 427 30. **Wilkins, M. J., N. C. VerBerkmoes, K. H. Williams, S. J. Callister, P. J. Mouser, H.**
 428 **Elifantz, A. L. N'Guessan, B. C. Thomas, C. D. Nicora, M. B. Shah, P. Abraham, M. S.**
 429 **Lipton, D. R. Lovley, R. L. Hettich, P. E. Long, and J. F. Banfield.** 2009. Proteogenomic
 430 monitoring of *Geobacter* physiology during stimulated uranium bioremediation. *Appl*
 431 *Environ Microb* **75**:6591-6599.
- 432 31. **Wu, L., L. Kellogg, A. Devol, J. Tiedje, and J. Zhou.** 2008. Microarray-based
 433 characterization of microbial community functional structure and heterogeneity in marine
 434 sediments from the gulf of Mexico. *Appl Environ Microb* **74**:4516-4529.
- 435 32. **Wu, L. Y., X. Liu, C. W. Schadt, and J. Z. Zhou.** 2006. Microarray-based analysis of
 436 subnanogram quantities of microbial community DNAs by using whole-community genome
 437 amplification. *Appl Environ Microb* **72**:4931-4941.
- 438 33. **Xu, M., W. Wu, L. Wu, Z. He, J. Van Nostrand, Y. Deng, J. Luo, J. Carley, M.**
 439 **Ginder-Vogel, T. Gentry, B. Gu, D. Watson, P. Jardine, T. Marsh, J. Tiedje, T. Hazen,**
 440 **C. Criddle, and J. Zhou.** 2010. Responses of microbial community functional structures to
 441 pilot-scale uranium in situ bioremediation. *ISME J* **4**:1060-1070.
- 442 34. **Yabusaki, S. B., Y. Fang, P. E. Long, C. T. Resch, A. D. Peacock, J. Komlos, P. R.**
 443 **Jaffe, S. J. Morrison, R. D. Dayvault, D. C. White, and R. T. Anderson.** 2007. Uranium
 444 removal from groundwater via in situ biostimulation: Field-scale modeling of transport and
 445 biological processes. *J Contam Hydrol* **93**:216-235.
- 446 35. **Zhou, J., M. Bruns, and J. Tiedje.** 1996. DNA recovery from soils of diverse composition.
 447 *Appl Environ Microb* **62**:316-322.
- 448 36. **Zhou, J., S. Kang, C. Schadt, and C. Garten.** 2008. Spatial scaling of functional gene
 449 diversity across various microbial taxa. *Proc Natl Acad Sci USA* **105**:7768-7773.

450 TABLE AND FIGURE LEGENDS

451 Table1 Groundwater geochemical data of samples selected for GeoChip analysis

452 Figure 1 Layout of the experimental plots at the Old Rifle uranium mill tailings site. Each plot had
 453 5 injection wells (open circles) perpendicular to groundwater flow, 4 monitoring wells (filled
 454 circles) down-gradient of acetate injection, and 1 monitoring well positioned upgradient of the
 455 injection wells (filled triangle). The 2004 experimental plot was maintained in Fe-reducing
 456 conditions and the 2005 experimental plot was driven to sulfate-reducing conditions by using
 457 different durations of biostimulation.

458 Figure 2 Hierarchical cluster analysis of all functional genes detected (a). Genes that were present
459 in at least three time points were used for cluster analysis. Results were generated in CLUSTER and
460 visualized using TREEVIEW. Red indicates signal intensities above background while black
461 indicates signal intensities below background. Brighter red colouring indicates higher signal
462 intensities. A total of 6 major groups were observed (b). The numbers equal groupings found
463 among the hybridization patterns.

464 Figure 3 Functional gene abundance in background well (B05), Fe-reducing well (M16) and shift
465 from Fe-reducing to sulfate-reducing wells (M21 and M24). The abbreviations are as follows: Org,
466 Organic contaminant degradation; Nred, Nitrogen reduction; Nit, Nitrification; Nfix, Nitrogen
467 fixation; Methane, Methane generation; Met, Metal reduction and resistance; DSR, Sulfate
468 reduction; Cfix, Carbon fixation; Cdeg, Carbon degradation.

469 Figure 4 Hierarchical clustering of c-type cytochrome genes. Red indicates signal intensities above
470 background while black indicates signal intensities below background. Brighter red colouring
471 indicates higher signal intensities. The bar of colors below the sample names indicates the average
472 signal intensities of each sample. Mantel test results indicated significant correlations between the
473 functional gene patterns and the U(VI) concentration ($P < 0.05$).

474 Figure 5 Canonical correspondence analysis (CCA) of total functional genes and geochemical data.

Table 1 Groundwater geochemical data of samples selected for GeoChip analysis

	Acetate (mM)	U(VI) (μ M)	Sulfate (mM)	Sulfide (mM)	Fe(II) (mM)	DO (mg/L)	pH	Conductivity (us/cm)	E _h (mV)
B05 7/27/06	0.00	0.91	6.62	0.000	0.063	0.33	7.04	2047	148
B05 9/19/06	0.00	1.00	7.52	0.000	0.018	0.32	6.92	2190	94
M16 9/5/06	2.34	0.52	7.38	0.003	0.0246	0.36	6.87	2431	84
M16 9/19/06	4.44	0.19	7.34	0.010	0.034	0.33	6.92	2659	11
M21 7/27/06	6.87	0.44	7.21	0.009	0.124	0.16	7.08	2936	33
M21 8/10/06	2.30	0.36	6.54	0.114	0.038	0.11	7.21	2465	-129
M24 7/27/06	2.10	0.24	7.05	0.004	0.127	0.1	7.02	2383	40
M24 8/10/06	0.83	0.50	5.80	0.096	0.013	0.2	7.19	2429	-141

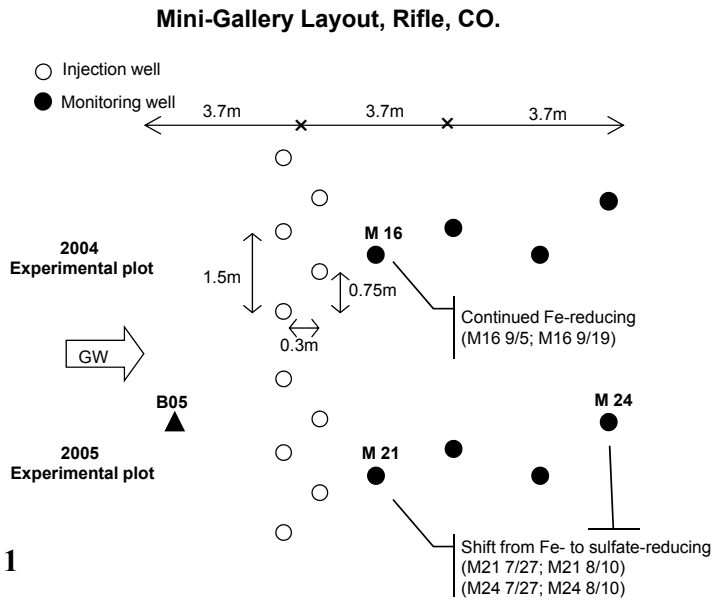
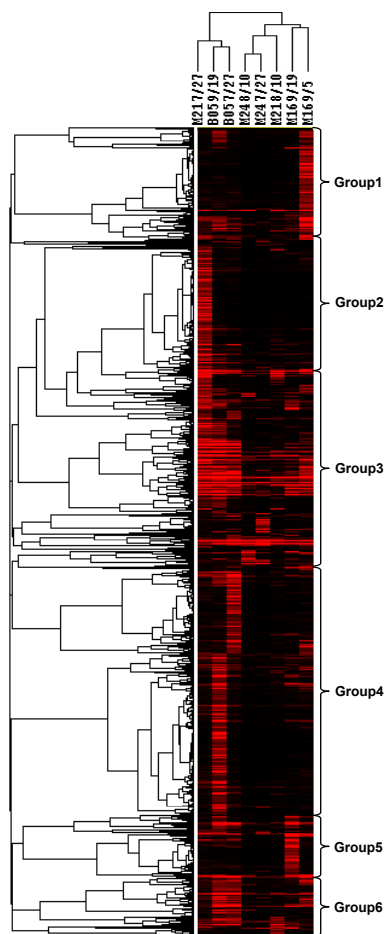


Figure 1

Figure 2 (a)



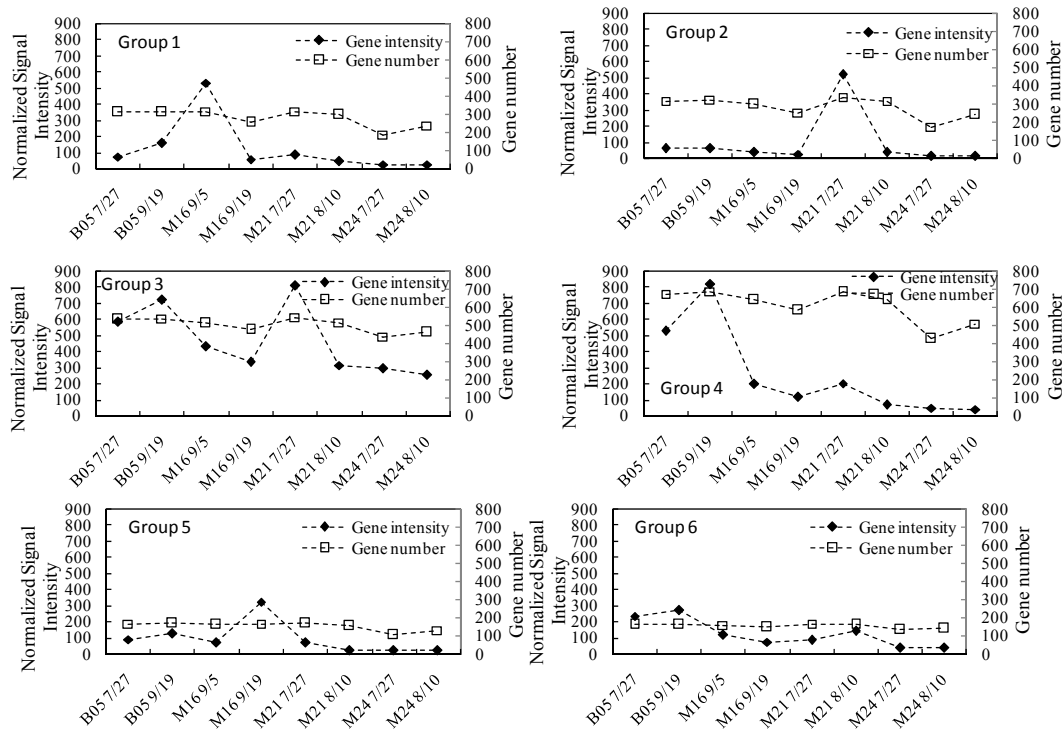


Figure 2 (b)

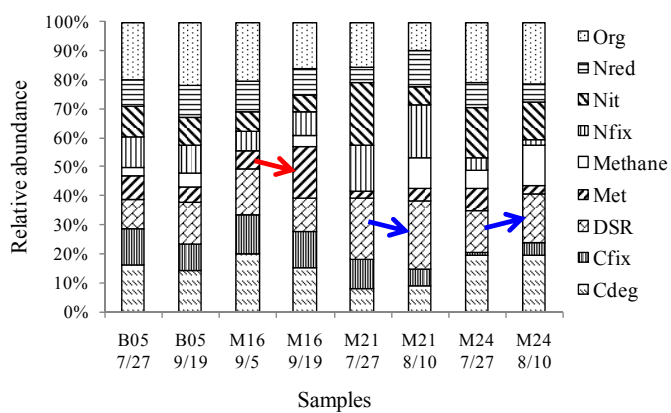


Figure 3

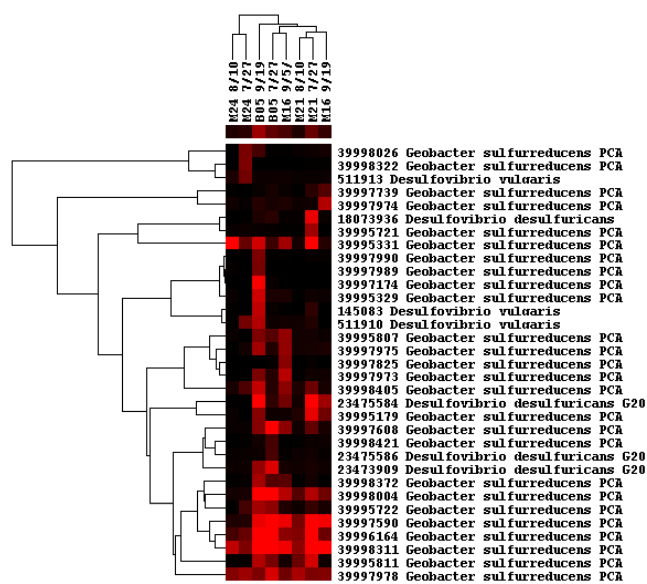


Figure 4

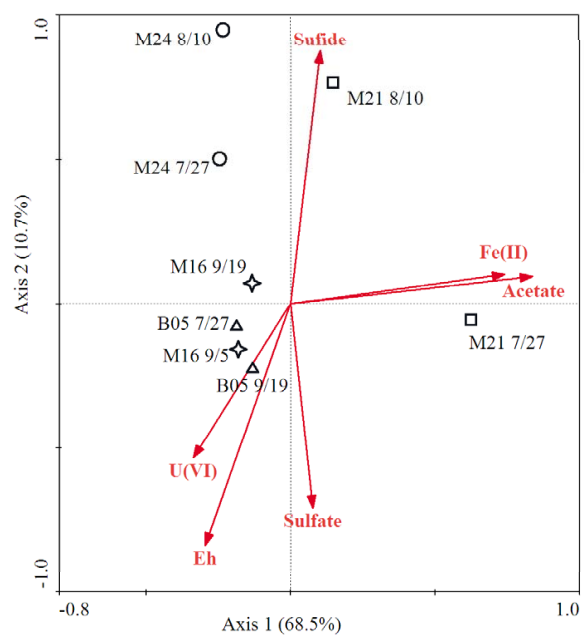


Figure 5